Constitutive models with Formative Hardening and Non-Linear Kinematic Hardening Rules for Simulation of Ratcheting

Shafiqul Bari and Tasnim Hassan*
Center for Nuclear Power Plant Structures, Equipment and Piping
North Carolina State University, Box 7908, Raleigh, NC 27695-7908, USA
thassan@eos.ncsu.edu

ABSTRACT

It is well known that the simulation of ratcheting responses under non-proportional loading histories depends primarily on the hardening rule of a constitutive model. The hardening rule is used to model the evolution of the yield surface caused by plastic loading. In reality, the shape of yield surface changes with progressive plastic loading. However, for the sake of simplicity, a common practice in modeling is to use the von-Mises yield surface and a non-linear kinematic hardening rule. An alternative approach would be to use a formative hardening rule that attempts to incorporate the yield surface shape change into modeling. In the paper, these two types of hardening rules are evaluated in terms of the simulation of ratcheting responses from a set of uniaxial and biaxial experiments.

I. INTRODUCTION

The modeling of cyclic plasticity responses is quite complex. Experimental studies demonstrate that the yield surfaces grow, translate as well as change shape with plastic loading. Some metals harden, while many others soften, during plastic cyclic loading. Moreover, the cyclic plasticity responses are history dependent. Most of the existing constitutive models fail to simulate these complex phenomena representatively as they assume idealized simple yield functions and hardening rules. In addition, most of the cyclic plasticity models for ratcheting simulations are developed and verified using data from limited or simple experiments. They are rarely tested against a wide variety of ratcheting responses to verify the generality of these models. Consequently, most of these constitutive models might predict a special class of ratcheting responses quite well, but fail to predict ratcheting responses in structures.

Although most metals cyclically harden or soften up to a certain number of cycles, they subsequently stabilize. Ratcheting strains, however, keep on accumulating with cycles even after the material stabilizes. The kinematic hardening (translation of the yield surface in stress space) is attributed to be the primary reason for ratcheting. Therefore, in order to develop and verify a basic model for ratcheting simulation, it is essential to study the ratcheting responses of stabilized materials. After achieving a robust model for ratcheting responses of cyclically stable materials, it can be extended to cyclically hardening and softening materials.

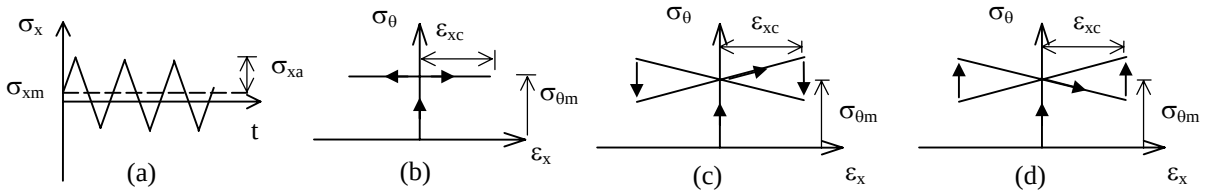

Fig 1.1 Loading histories; (a) Uniaxial stress cycles, (b) Axial strain cycle with constant pressure, (c) biaxial bow-tie cycle, (d) biaxial reverse bow-tie cycle.

A broad set of quasi-static ratcheting data, which include uniaxial to complex biaxial ratcheting responses of stabilized carbon steels, have been developed by Hassan and Kyriakides [1992], Hassan et al. [1992] and Corona et al. [1996]. These data are used to evaluate the performance of the models considered in this study. The loading histories of the experiment set are shown in Fig. 1.1. The history in Fig. 1.1a, which results in ratcheting of axial strains, involves axial stress controlled cycles with a mean stress. The loading history in Fig. 1.1b involves axial strain cycles in the presence of a constant

* The corresponding author

internal pressure. This history results in ratcheting of the circumferential strain. The so-called *bow-tie* and *reverse bow-tie* loading histories shown in Fig. 1.1c and d also result in circumferential strain ratcheting.

The modeling for ratcheting simulations under uniaxial loading is inherently different from that under multiaxial loading. Also, the role of various parameters differs considerably depending on the loading condition. Most of the existing models apparently fail to appreciate this distinction. The parameter determination schemes followed by these models are, sometimes, incomplete and vague. As a result, these models are not general and rarely perform representatively for varied loading conditions. It is, therefore, essential to scrutinize the parameter determination schemes of various models for ratcheting simulation and evaluate their performance against a broad set of experimental responses.

The modeling schemes for the cyclic plasticity and ratcheting simulations can be classified into two types: *coupled* and *uncoupled*. In the *coupled* modeling scheme, the plastic modulus calculation is coupled with the kinematic hardening rule through the consistency condition of the yield surface (Prager [1956]). Consequently, in uniaxial loading condition, the kinematic hardening rule is effectively used to calculate the plastic modulus, as the evolution direction is constant in this case. In multiaxial loading condition, however, the hardening rule affects both the plastic modulus and the evolution direction. If hardening rule parameters are calibrated from uniaxial loading responses only, as has been done in many existing coupled models, the hardening rule is basically designed for better representation of the plastic modulus, which undermines its role in describing the direction of the yield surface evolution. Because of this approach in modeling, many popular coupled models perform well in one type of loading condition while fail in others. For example, in the Chaboche (1991) and the Ohno-Wang (1993) models, all parameters are determined using uniaxial responses. Bari and Hassan [2001a] demonstrate that these models perform reasonably well in simulating uniaxial ratcheting responses, but overpredict consistently for all biaxial ratcheting responses considered.

In the *uncoupled* modeling scheme, on the other hand, the plastic modulus may be indirectly influenced by the kinematic hardening rule but its calculation does not depend on it. Therefore, the hardening rule parameters can be calibrated from multiaxial loading conditions without having any effect on the simulation by the model in uniaxial loading condition. Bari and Hassan [2000b] demonstrates that the Chaboche kinematic hardening rule in the modified Dafalias-Popov uncoupled scheme performs well in for both all type of loading conditions shown in Fig. 1. However, the determination of the kinematic hardening rule parameter can be somewhat subjective in uncoupled modeling scheme, unless simple hardening rules are used.

In order to achieve better simulations in both uniaxial and multiaxial cases, another approach is to introduce special multiaxiality terms or parameters in the kinematic hardening rule for a coupled model. These terms and parameters should remain dormant under uniaxial loading (or do not take part in the plastic modulus calculation), but play an important role in defining representative yield surface translation and thus plastic strain rate directions. As the actual yield surface shape deforms during plastic loading (Phillips and Tang, 1972, Phillips and Lee, 1979), the lack of exactness introduced in the modeling through invariant yield surface shape assumption is compensated to some extent by calibrating these parameters using multiaxial ratcheting responses. Using this concept, Bari and Hassan [2000c] introduces an improved kinematic hardening rule by of appropriately blending the Armstrong-Frederick (1966) and the Burlet and Cailletaud (1986) rules. This improved kinematic hardening rule is used in the decomposed hardening framework of the Chaboche (1991) model. It includes a parameter d' that does not take part in the plastic modulus calculation, but produces meaningful influence on the yield surface translation under multiaxial loading. As a result, uniaxial ratcheting simulations by this model are exactly the same as those by the Chaboche (1991) model, regardless of the value of d'. Figure 1.2 shows the simulations by this improved coupled model for all the loading conditions of Fig. 1.1. When d' is calibrated using a biaxial ratcheting experiment (Fig 1.2.c), simulations by this rule manifest improvement for the biaxial ratcheting responses considered (see Figs. 1.2c to 1.2f). The authors have critically evaluated a number of coupled and uncoupled models against the same set of uniaxial and biaxial ratcheting responses in three successive papers (Bari and Hassan, 2000a,b and c). Among all these models, this kinematic hardening rule performs the best in simulating the whole set of responses considered. Moreover, the parameter determination scheme of this model is simple and systematic.

The authors like to emphasize the fact that the calibration of the new parameter in the modified rule using a biaxial ratcheting experiment merely tries to compensate for the lack of exactness of the model introduced by various assumptions. As a result, applicability of the model to multiaxial loading histories depends strongly on the ratcheting response used for the parameter calibration. In addition, all the models discussed so far consider the von-Mises yield surface as the yielding boundary and also, as the plastic potential surface. But in reality, the yield surface translates as well as deforms during plastic loading (Phillips and Tang [1972], Phillips and Lee [1979]). The incompleteness, thus, introduced in the modeling bars the classical cyclic plasticity models from being successful in the general multiaxial loading conditions. Therefore, investigations have been conducted in paper to incorporate the anisotropically deformed yield surface in the cyclic plasticity modeling scheme (formative hardening rule).

From the experimental trends observed for the shapes of the yield surface, Phillips and Tang [1972] put forward a qualitative model of the translation and distortion of the yield surfaces during plastic loading. Ortiz and Popov [1983], Eisenberg and Yen [1981,1984], Ishikawa and Sasaki [1988], and Wegener and Schlegel [1996] propose analytical and

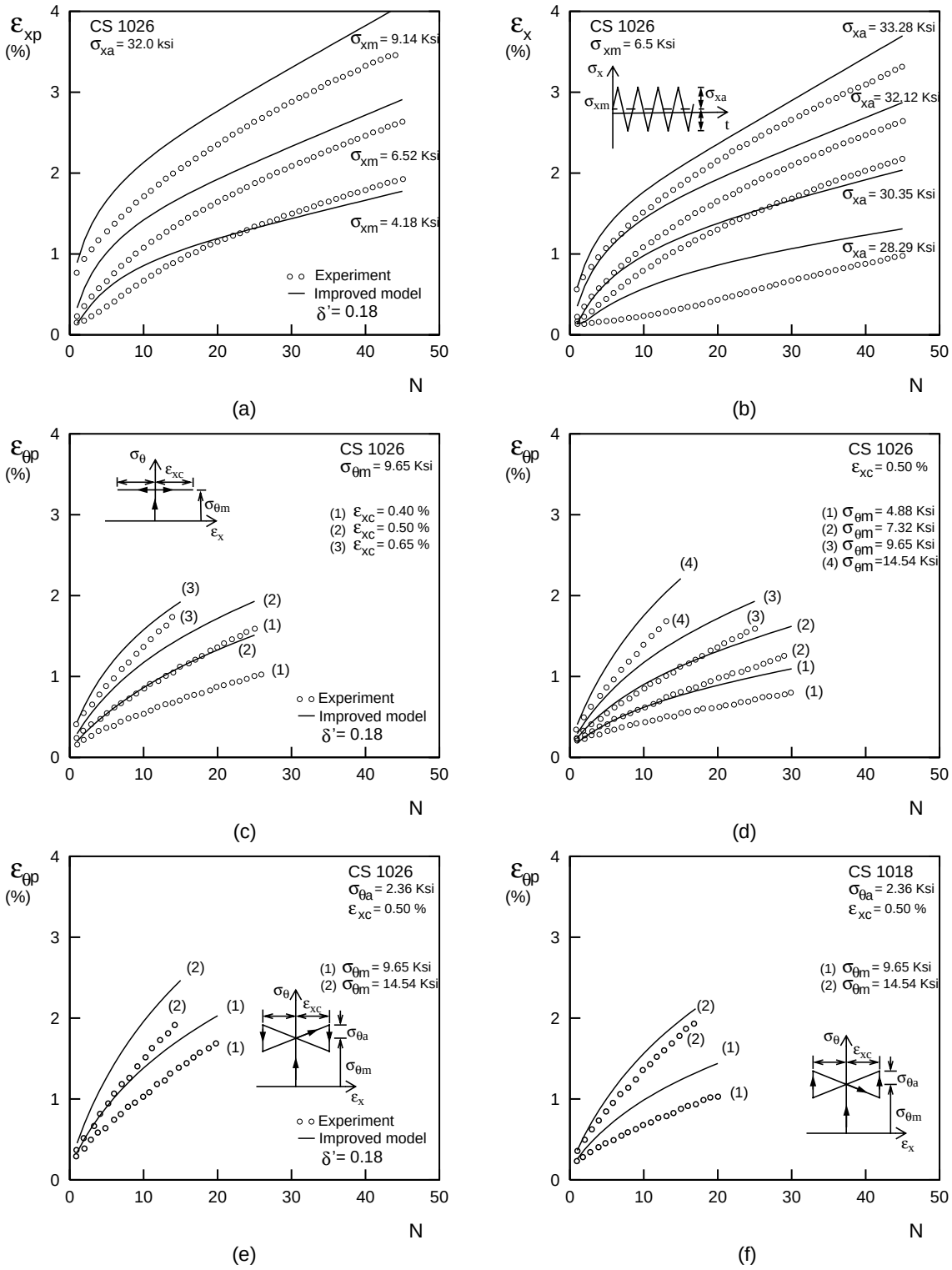

Fig. 1.2. Ratcheting predictions by the Improved model (Eq. 16). (a,b) Axial strain at positive stress peaks from uniaxial cycles, (c,d) circumferential strain peaks from axial strain cycles with constant pressure, (e,f) circumferential strain peaks from bow-tie and reverse bow-tie cycles. Experiments are from Hassan and Kyriakides (1992), Hassan et al. (1992) and Corona et al. (1996).

numerical modeling schemes to implement the yield surface shape change observations of Phillips and Tang [1972]. After careful scrutiny of these modeling schemes, it has been observed that most of these models use complex and numerically extensive schemes with higher order state tensors. As a result, these models become less attractive (in some cases, impractical) for implementation with a cyclic plasticity model.

. Shiratori and his co-workers (Yoshida et. al [1977], Shiratori et. al [1979]), on the other hand, propose a so-called equi-plastic-strain surface that can be used as the plastic potential surface. The formulation for the equi-plastic-strain surface is simpler compared to other deformed yield surface formulations. This study demonstrates the basic methodology and promise in incorporating the equi-plastic-strain surface as the plastic potential surface into the cyclic plasticity modeling.

II. RATCHETING SIMULATION WITH FORMATIVE HARDENING RULE

II. 1. Equi-plastic-strain surface

In classical plasticity modeling, the derivative of a scalar surface called the plastic potential surface gives the direction of plastic flow at the stress point. In most of the cyclic plasticity models (including the ones discussed in this paper so far), the yield surface is employed to accomplish two purposes. Firstly, it defines the boundary between elastic and plastic deformations. It also acts as the plastic potential surface in the flow rule. It is demonstrated in the introduction that the modeling of the anisotropically-deformed yield surfaces are complex, numerically extensive and in many cases, impractical. Realizing the limitations of using these anisotropically-deformed yield surface in the cyclic plasticity modeling, Yoshida et. al [1977] and Shiratori et. al [1979] propose a so-called equi-plastic-strain surface that can act as the plastic potential surface. The yield surface still defines the elastic-plastic boundary. The motivation behind using the equi-plastic-strain surface over its yield surface counterpart is that the equi-plastic-strain surfaces have been experimentally observed to assume relatively simpler shapes when defined in the Ilyushin [1954] stress space. As a result, the numerical modeling of the plastic potential surface is less involved and requires fewer parameters to be determined from experimental responses.

Yoshida et. al [1977] and Shiratori et. al [1979] define the equi-plastic-strain surface as the locus of equal plastic strains measured from the recent unloading point in the stress space. Figure 2.1 shows a qualitative diagram of the equi-plastic-strain surface in the Ilyushin [1954] vector stress space. For any loading path OSQ_iP_i, after unloading at S, the loading path SQ_i (for i = 1,2,....n) is the elastic reloading stage within the subsequent yield surface where no plastic strains accumulate. The point Q_i (for i = 1,2,....n) falls on the initial yield surface F_0. If the accumulated plastic strains

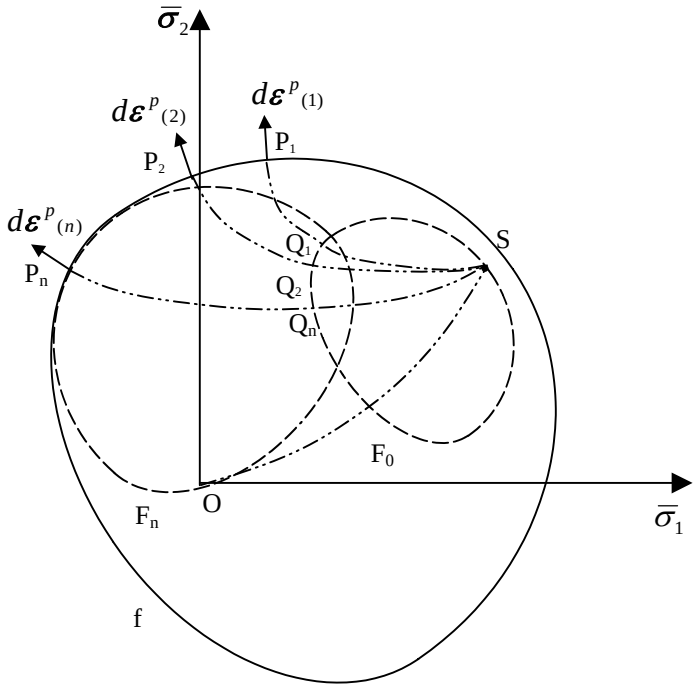

Fig. 2.1 Qualitative equi-plastic-strain surface in Ilyushin [1954] vector stress space

$$p = \int_{(Q_i)}^{(P_i)} \left| d\boldsymbol{\varepsilon}^p \right|, i = 1,2,.....n \qquad (2.1)$$

for paths Q_iP_i are equal, then the locus of these equal plastic strain points P_i (for i = 1,2,....n) approximately forms a closed surface f called the equi-plastic-strain surface. It should be observed that, for $p \cong 0$, the equi-plastic-strain surface and the yield surface are the same. However, at the loading point P_n, the subsequent yield surface F_n touches the equi-plastic-strain surface f. Therefore, both surfaces have the same normal at the loading points, which signifies that the equi-plastic-strain surface can be considered as a valid plastic potential surface. The plastic strain increment can be derived from the principle of maximum plastic work as follows:

$$d\boldsymbol{\varepsilon}^p = d\lambda(grad\, f). \qquad (2.2)$$

Yoshida et. al [1977] and Shiratori et. al [1979] have conducted several equi-plastic-strain surface experiments on Brass, Aluminum alloy, Ni-Cr Mo steel and Mild steels. These experiments demonstrate that the equi-plastic-strain surfaces match experimentally observed shapes of the yield surfaces for $p \cong 0$,i.e., a rounded corner in the loading side and a flattening corner at the rear side. The shape of the subsequent equi-plastic-strain surfaces gradually approach a concentric isotropic hardening hyper-sphere with increasing plastic strains. The equi-plastic-strain surfaces are found to be symmetric with respect to the radial line passing through the unloading point. Shiratori et. al [1979] also demonstrate from a set of experiments (see Fig. 3 and 4 in the reference) that the normal directions to the equi-plastic-strain surface at stress points do match the experimentally observed directions of plastic strain increments. A qualitatively description of the evolution of the equi-plastic-strain surfaces with plastic loading is shown in Fig. 2.2.

In an effort to simulate the experimentally observed shapes, Shiratori et. al [1979] propose an expression for the equi-plastic-strain surfaces in the moving stress space $\bar{\boldsymbol{\sigma}}'_{\acute{e}}$ of the fixed Ilyushin space $\bar{\boldsymbol{\sigma}}_i$ (shown in Fig 2.2). Although this model is demonstrated to perform well in a number of non-proportional loading cases including two types of non proportional cyclic loading histories, it makes some assumptions that limits the use of this model in general multiaxial loading conditions, especially in simulations of the ratcheting responses. These limitations are: (i) It uses the equivalent (von-Mises) stress-strain values to represent the general multiaxial stress-strain states. This idealization undermines the effect of the loading history in ratcheting responses under general multiaxial loading. (ii) It ignores the Bauchinger effect in uniaxial cyclic loading, which is critical for uniaxial ratcheting responses. (iii) It assumes that the equi-plastic-strain surfaces in

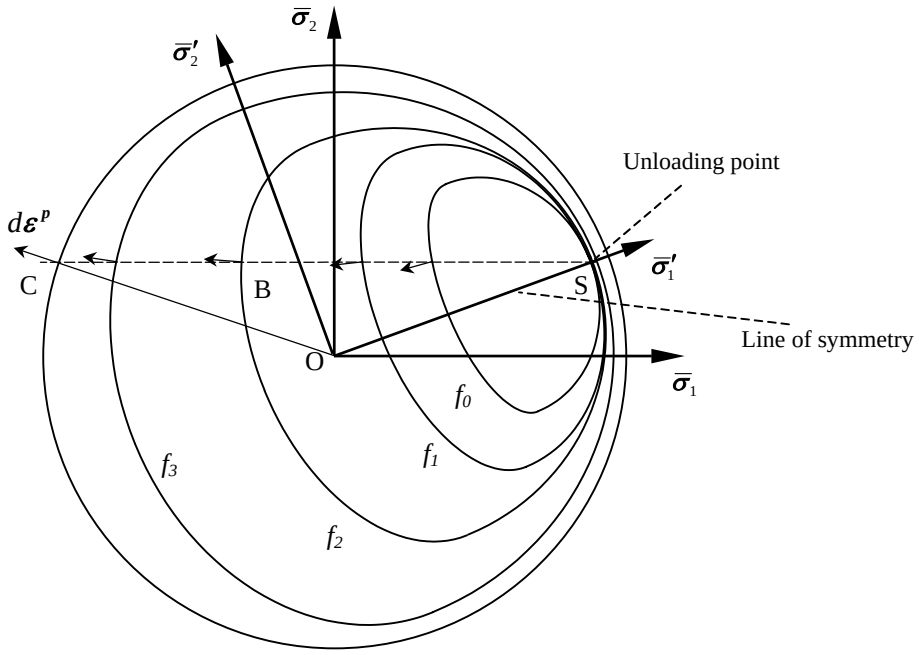

Fig. 2.2. Subsequent equi-plastic-strain surfaces and plastic strain increment directions

Ilyushin stress space are symmetric with respect to a radial line passing through the unloading point. It should be realized that the plastic potential surface should be smooth enough to have unique normal direction at all loading points. Therefore, if the plastic potential surface is symmetric with respect to a line, the normal directions at the points where the symmetry line touches the potential surface are collinear with the line of symmetry. In all the experiments presented by Shiratori et. al [1979], the unloading points lie sufficiently close to the isotropic hyper-sphere (see Fig. 4 and Fig. 18 in the reference) so that the normal directions at the unloading points are very close to be radial. As a result, the symmetry lines appear to pass through the origin in all these experiments. However, in case of an unloading point far away from the isotropic hyper-sphere, the normal directions are not expected to be radial. If we observe the variation of the normal directions along the path SBC in Fig. 2.2, it is clear that the normal directions start from being radial at S and then, gradually change to become radial again when it touches the isotropic hyper-sphere at C. Therefore, if the unloading occurs at points S or C, the symmetry line is expected to be radial or very close to it. However, if unloading occurs at some point like B, the line of symmetry would be different from the radial line through B. (iv) The methodology for the determination of plastic modulus and other parameters presented in Shiratori et. al [1979] can not be applied in combined stress-strain controlled loading conditions.

Regardless of these limitations, the Shiratori et. al [1979] model demonstrates promise and success in putting forward a simpler modeling scheme for incorporating the effect of yield surface shape change in the cyclic plasticity modeling. In this study, efforts have been made to present a cyclic plasticity modeling scheme that uses the equi-plastic-strain surface as the plastic potential surface and tries to address the limitations of the Shiratori model to improve the simulations of ratcheting responses in general multiaxial loading. Two different modeling schemes are studied. Performances of these models are evaluated against a set of constant pressure biaxial ratcheting experiments (Fig 1.1b). These modeling schemes and their results are presented below.

II.2. Coordinate system

The equi-plastic-strain surfaces are represented in the five-dimensional Cartesian deviatoric stress and plastic strain vector spaces as introduced by Ilyushin [1954]. Stress and plastic strain vector components in the spaces $\bar{\sigma}_i$ and $\bar{\varepsilon}_i$ (i = 1,2,....5) are given as follows:

$$\bar{\sigma}_1 = \tfrac{3}{2} S_{11},\ \bar{\sigma}_2 = \tfrac{\sqrt{3}}{2}(S_{11} + 2S_{22}),\ \bar{\sigma}_3 = \sqrt{3} S_{12},\ \bar{\sigma}_4 = \sqrt{3} S_{23},\ \bar{\sigma}_5 = \sqrt{3} S_{32}; \qquad (2.3)$$

$$\bar{\varepsilon}_1^{\,p} = \varepsilon_{11}^{\,p},\ \bar{\varepsilon}_2^{\,p} = \tfrac{1}{\sqrt{3}}(\varepsilon_{11}^{\,p} + 2\varepsilon_{22}^{\,p}),\ \bar{\varepsilon}_3^{\,p} = \tfrac{2}{\sqrt{3}} \varepsilon_{12}^{\,p},\ \bar{\varepsilon}_4^{\,p} = \tfrac{2}{\sqrt{3}} \varepsilon_{23}^{\,p},\ \bar{\varepsilon}_5^{\,p} = \tfrac{2}{\sqrt{3}} \varepsilon_{31}^{\,p} \qquad (2.4)$$

where S_{ij} and $\varepsilon_{ij}^{\,p}$ are deviatoric stress and plastic strain tensor components in the three-dimensional Cartesian coordinate system respectively. In the Ilyushin space, the stress and the plastic strain vectors are given as

$$\bar{\sigma} = \sum_{i=1}^{5} \bar{\sigma}_i \bar{e}_i \quad \text{and} \quad \bar{\varepsilon}^{\,p} = \sum_{i=1}^{5} \bar{\varepsilon}_i^{\,p} \bar{e}_i \qquad (2.5)$$

where $\bar{e}_i$ are the unit vectors along the Ilyushin axes.

II.3. Flow rule

Upon considering the equi-plastic-strain surface as the plastic potential surface, the plastic strain increment can be derived from the normality rule and the principal of maximum plastic work as follows:

$$d\bar{\varepsilon}^{\,p} = d\lambda\, \bar{n}_G = \frac{1}{H}(\bar{n}_G \cdot d\bar{\sigma})\bar{n}_G \qquad (2.6)$$

where $\bar{n}_G = \dfrac{\partial f / \partial \bar{\sigma}}{\left| \partial f / \partial \bar{\sigma} \right|}$, f is the equi-plastic-strain surface and H is the plastic modulus.

II.4. Model I

(a) Equi-plastic-strain surface

Both Yoshida et. al [1977] and Shiratori et. al [1979] propose two similar type of expressions of the equi-plastic-strain surface in the moving stress space $\bar{\sigma}'_{\hat{e}}$ of the fixed Ilyushin space $\bar{\sigma}_i$. However, they do not provide any basis for their selection. On the other hand, Kurtyka and Zyczkowski [1996] present a general form for defining any anisotropically deformed surface in the Ilyushin vector space. In this study, a special case of this general form is adopted to describe the shape of the equi-plastic-strain surface. With the assumption that the equi-plastic-strain surface is symmetric with respect to a

direction $\bar{\sigma}_{PR}$, the expression for the equi-plastic-strain surface is proposed in this study as follows:

$$\frac{(\bar{\sigma}_1' - \sigma_0^*)^2}{R_1^2 + 2d_1(\bar{\sigma}_1' - \sigma_0^*) - d_1^2} + \sum_{k=2}^{5} \frac{(\bar{\sigma}_k' - v_Y)^2}{R_k^2} = 1 \qquad (2.7)$$

where $R_1 = (\sigma_N - \sigma_M)/2$, $R_k = \sigma_B - \sigma_C^*$, $d_1 = \sigma_N - \sigma_0^* - R_1$.

All the parameters and variables in Eq. 2.7 are shown in Fig. 2.3. As adopted by Shiratori et. al [1979], the expressions for σ_0^* and σ_C^* are assumed to depend on the accumulation of plastic strain from unloading and $(\delta_p + \delta_q)$ as follows:

$$\sigma_0^* = C_1(\delta_p + \delta_q)e^{-m_1(\rho_* + dp)} \text{ and } \sigma_C^* = C_2(\delta_p + \delta_q)e^{-m_2(\rho_* + dp)} \qquad (2.8)$$

where $\delta_p = v_b + \sigma_B - \sigma_N$, $\delta_q = \sigma_M - v_b + \sigma_B$ and is ρ_* the accumulated plastic strain after unloading. It should be noted that the equi-plastic-strain surface in this model gradually approaches a bounding surface for very large ρ_*.

(b) Plastic modulus H

It has been demonstrated in Bari and Hassan [2000b] that the plastic modulus calculation scheme by Dafalias and

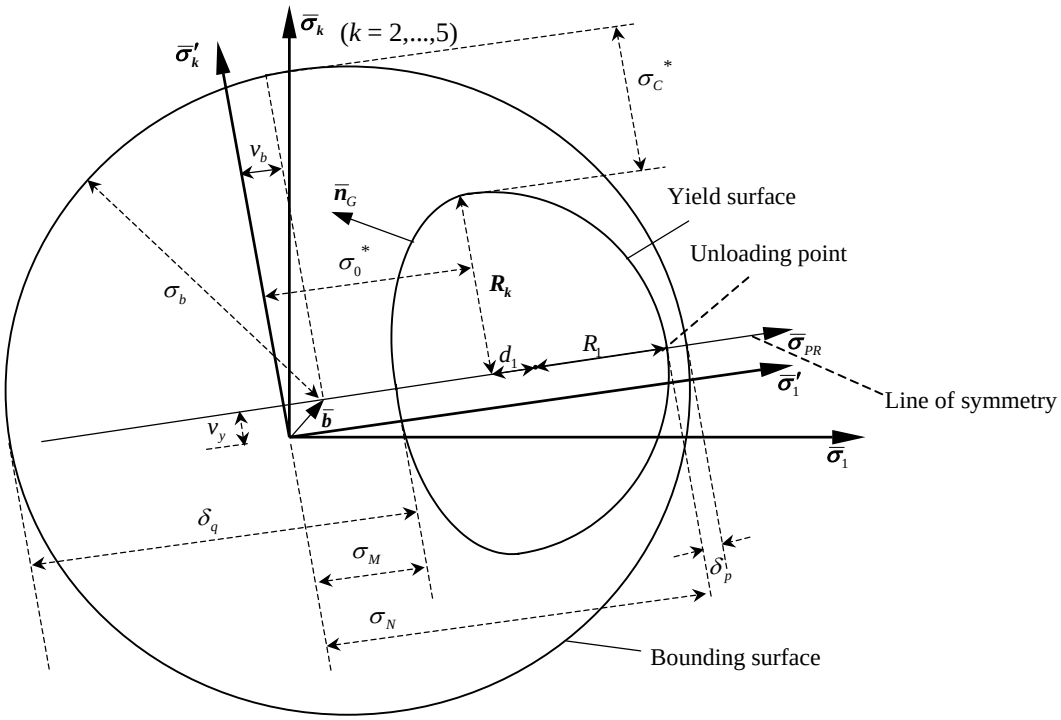

Fig. 2.3. Equi-plastic-strain surface I in the moving stress space $\bar{\sigma}_i'$ of the Ilyushin space

Popov [1976] is successful in simulating the ratcheting responses when used with appropriate hardening rule. Therefore, the same scheme is also adopted in this study to calculate the plastic modulus as follows:

$$H = E_0^p + h\left(\frac{\delta}{\delta_{in} - \delta}\right), \; h = \frac{a}{1 + b\left(\frac{\delta_{in}}{2\sigma_B}\right)^m} \qquad (2.9)$$

where $\delta = \left|\bar{\sigma}_B - \bar{\sigma}\right|$ and $\bar{\sigma}_B = \sigma_B \bar{n}_G + \bar{b}$. The δ_{in} is the initial δ after unloading, E_0^p is the plastic modulus of the

bounding surface, $\bar{\sigma}_B$ is the image point of $\bar{\sigma}$ on the bounding surface and $\bar{b}$ is the bounding surface center. The parameters *a*, *b* and *m* are determined from a uniaxial ratcheting test as described by Bari and Hassan [2000b].

(c) Hardening rule

It has been observed in experiments from Shiratori et. al [1979] that δ_p and δ_q decrease with the increase in plastic strain value. With them, $\sigma_0{}^*$ and $\sigma_C{}^*$ also decrease according to Eq. 2.8 and the equi-plastic-strain surface gradually approaches the bounding surface. When δ_p and δ_q become zero, the equi-plastic-strain surface converges with the bounding surface. This hardening mechanism of the equi-plastic-strain surface is modeled in this study as follows:

$$d\sigma_M = -K\delta_q + dv_b,\ d\sigma_N = K\delta_p + dv_b\ ,\ dv_b = -E_0{}^p dp\ . \qquad (2.10)$$

It should be observed in Eq. 2.10 that the bounding surface does not grow in size, but translates along the negative $\bar{\sigma}_{PR}$ direction. The magnitude of the scalar *K* is determined from the consistency condition at each loading increment.

(d) Symmetry direction

The experimental data from Shiratori et. al [1979] shows that the equi-plastic-strain surfaces appear to be symmetric with respect to a radial line. However, there is no experimental data available showing the shapes of the equi-plastic-strain surface when unloading occurs far away from the bounding surface. In order to hold the basic premise that the equi-plastic-

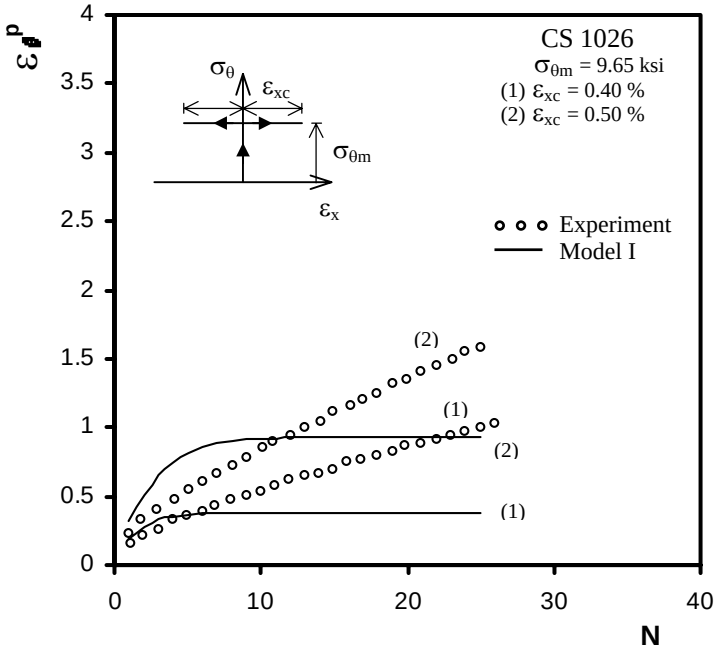

Fig. 2.4. Biaxial ratcheting predictions by model I and experiments from Hassan and Kyriakides [1992].

strain surface can be used as a plastic potential surface, the line of symmetry for the equi-plastic-strain surface has to be along the plastic strain increment (or normal to the equi-plastic-strain surface) at the unloading stress point. Therefore, in this study, it is assumed that the line of symmetry is along the normal direction at the unloading point, i.e.,

$$\bar{\sigma}_{PR} = \bar{n}_G \text{ (at the unloading point)} \qquad (2.11)$$

(e) Ratcheting simulations

The performance of the above mentioned modeling scheme is evaluated against some biaxial ratcheting responses from Hassan and Kyriakides [1992] on stabilized carbon steels where cyclic axial strains are applied on straight pipe with steady internal pressure (see loading history (b) in Fig. 1.1). The material constants C_1, C_2, m_1 and m_2 that define the

characteristic values for $\sigma_0{}^*$ and $\sigma_C{}^*$ are supposed to be determined from equi-plastic-surface experiments in multiaxial loading condition according to Shiratori et. al [1979]. As there is no experimental data available on the shape of the equi-plastic-strain surface in stabilized carbon steels, these parameters are selected from a constant pressure biaxial ratcheting experiment in this study. Fig. 2.4 shows the simulation of ratcheting responses by this model along with the experimental responses under biaxial loading condition. The parameters used are:

$C_1 = 0.35$, $C_2 = 0.40$, $m_1 = 310$ and $m_2 = 210$.

The simulated accumulation of the hoop strains from this model tends to stabilize after some ratcheting during a couple of initial cycles. The predicted ratcheting responses for both axial strain amplitudes with the same internal pressure behave in a similar manner. This deviation of ratcheting responses from experimental responses can be attributed to the assumption that the line of symmetry is along the plastic strain increment at the unloading point (Eq. 2.11). With this assumption, this symmetry direction gradually flattens until it becomes parallel to the $\bar{\sigma}_1$ direction when the hoop strain component of plastic strain increment becomes zero. As a result, shakedown of ratcheting responses occurs.

II.5. Model II

In order to gain a better perspective on the use of equi-plastic-strain surface with the uncoupled modeling scheme for ratcheting simulations, another variation of the equi-plastic-strain surface and corresponding hardening rule is examined in this study. This modeling scheme (model II) differs from the model I in three key aspects: the symmetry direction, the plastic modulus *H* calculation, and the bounding surface evolution.

(a) Symmetry direction

Although it is argued in model I that the symmetry direction may not necessarily pass through the origin of the Ilyushin vector stress space in all loading histories, it has been observed in the experiments by Shiratori et. al [1979] that the

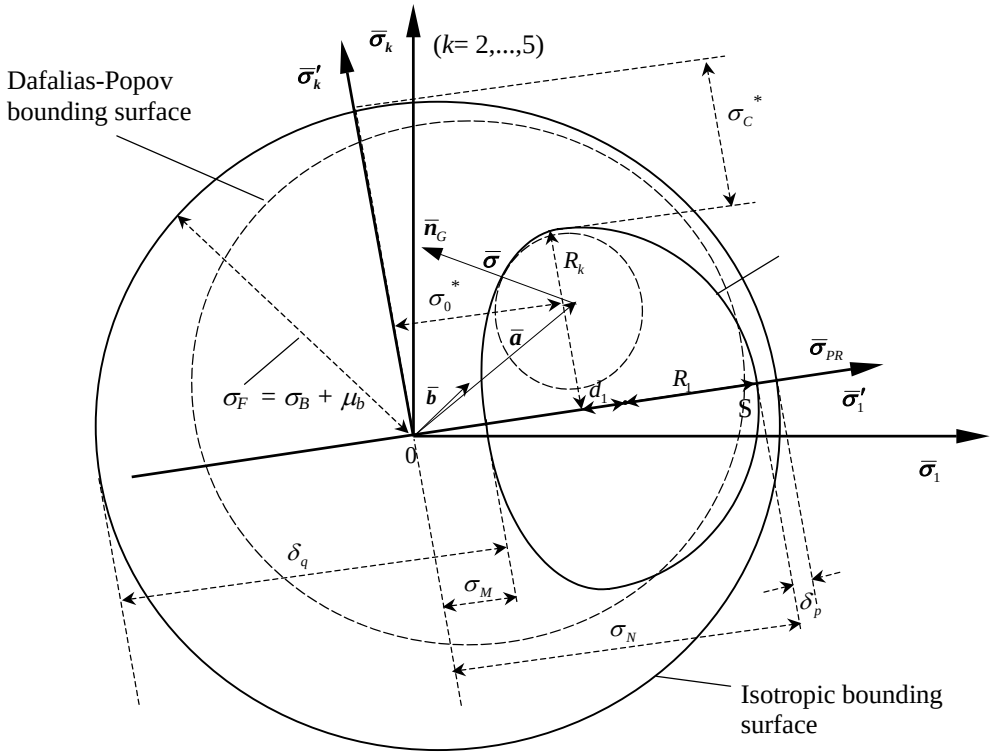

Fig. 2.5. Equi-plastic-strain surface II in the moving stress space $\bar{\sigma}'_i$ of the Ilyushin space

equi-plastic-strain surfaces tend be symmetric with respect to a radial line. It should be noted that, for the ratcheting experiments considered in this study to evaluate models I and II, enough plastic strains are accumulated in each cycle to bring

the unloading points sufficiently close to the bounding surface. For these experiments, the direction of the plastic strain increments (normals to the equi-plastic-strain surface) at the unloading points also are tend very close to radial. Therefore, in model II, the symmetry direction is considered to be the direction of the radial line passing through the unloading point (OS direction in Fig. 2.5).

(b) Equi-plastic-strain surface

In model II, the equi-plastic-strain surface is proposed to be symmetric with respect to the direction $\bar{\sigma}_{PR}$, as follows:

$$\frac{(\bar{\sigma}_1' - \sigma_0^*)^2}{R_1^2 + 2d_1(\bar{\sigma}_1' - \sigma_0^*) - d_1^2} + \sum_{k=2}^{5} \frac{(\bar{\sigma}_k')^2}{R_k^2} = 1 \qquad (2.12)$$

where $R_1 = (\sigma_N - \sigma_M)/2$, $R_k = \sigma_F - \sigma_C^*$, $d_1 = \sigma_N - \sigma_0^* - R_1$, $\sigma_F = \sigma_B + \mu_b$.
All the parameters and variables in Eq. 2.12 are illustrated in Fig. 2.5. The new parameter μ_b is the increase in size of the isotropic bounding surface during plastic loading from its original size σ_b. The expressions for σ_0^* and σ_C^* are assumed to depend on the accumulation of plastic strain after preloading and $(\delta_p + \delta_q)$ as follows:

$$\sigma_0^* = C_1(\delta_p + \delta_q)e^{-m_1(\rho_* + dp)} \text{ and } \sigma_C^* = C_2(\delta_p + \delta_q)e^{-m_2(\rho_* + dp)} \qquad (2.13)$$

where $\delta_p = \sigma_F - \sigma_N$, $\delta_q = \sigma_M + \sigma_F$ and ρ_* is the accumulated plastic strain after unloading.

(c) Plastic modulus H

The Dafalias and Popov [1976] plastic modulus calculation scheme (Eq. 5.13) is also adopted in this model. However, an additional Dafalias-Popov type kinematic bounding surface is introduced in this model as shown in Fig. 2.5 where, $\bar{b}$ is the center of the kinematic bounding surface. The image point of $\bar{\sigma}$ on the kinematic bounding surface is used as a measure of δ in Eq. 5.13. The same parameter determination scheme as used in Eq. 5.13 is adopted in model II as well.

(d) Hardening rule

In this model, the equi-plastic-strain surface gradually approaches the concentric isotropic bounding surface, which also grows in all direction with plastic loading. When δ_p and δ_q become zero, the equi-plastic-strain surface converges with the isotropic bounding surface. This hardening mechanism of the equi-plastic-strain surface is modeled as follows:

$$d\sigma_M = -K\delta_q + dv_b,\ d\sigma_N = K\delta_p + dv_b,\ d\mu_b = E_0^p dp. \qquad (2.14)$$

The kinematic bounding surface center $\bar{b}$ grows according to the evolution model proposed by Seyed-Ranjbari [1986] (also Hassan and Kyriakides [1994]) where $\bar{a} = \bar{\sigma} - \sigma_0 \bar{n}_G$ in this model. The readers are referred to Eqs. 6 and 7 of Bari and Hassan [2000b] for expressions of this evolution. The magnitude of the scalar *K* in Eq. 2.14 is determined from the consistency condition at each loading increment.

(e) Ratcheting simulations

The performance of the modeling scheme II is also evaluated against the same set of biaxial ratcheting responses as used in evaluating model I. The same guidelines to determine material constants C_1, C_2, m_1 and m_2 as adopted in model I are applied in this model. Fig. 2.6 shows the simulation of ratcheting responses by model II with parameters:

$C_1 = 0.36$, $C_2 = 0.42$, $m_1 = 310$ and $m_2 = 210$.

The simulated ratcheting responses for all axial strain amplitudes show an almost constant rate of ratcheting. For initial cycles, ratcheting simulations match the experimental responses reasonably, but fail to represent the ratcheting rates observed in the experiments for higher cycles (see Fig. 2.6). In addition, the changes in the ratcheting rates observed with different axial strain amplitudes in the experiments of Fig. 2.6 are not reproduced by model II.

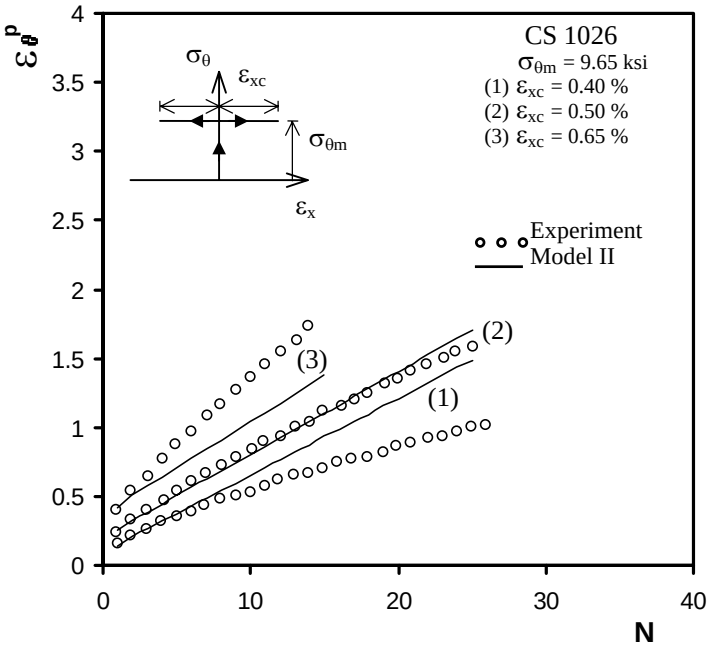

Fig. 2.6. Biaxial ratcheting predictions by model II and experiments from Hassan and Kyriakides [1992].

III. CONCLUSION AND DISCUSSIONS

Pioneering experimental by Phillips and his co-workers [1972,1979,1984] have demonstrated that the yield surfaces undergo both translation and distortion during plastic loading. The ensuing shapes of the yield surfaces are quite complex and different from the shapes of the von-Mises yield surfaces. As a result, cyclic plasticity models with the von-Mises yield surface rarely perform well for general multiaxial loading conditions. This limitation introduced by the isotropic von-Mises yielding assumption in ratcheting simulation models can be compensated to some degree by calibrating some of the kinematic hardening parameters using multiaxial ratcheting responses as has been demonstrated in the imroved coupled model by Bari and Hassan [2000c]. However, the generality of this methodology is yet to be validated. Therefore, in this study, efforts have been made to evaluate the prospect and potentials of incorporating the anisotropic deformation of the yield surface in cyclic plasticity modeling in order improve the ratcheting simulations in multiaxial, nonproportional loading conditions.

From the experimental trends observed, Phillips and Tang [1972] put forward a qualitative model of the translation and distortion of the yield surfaces during plastic loading. Ortiz and Popov [1983], Eisenberg and Yen [1981,1984], Ishikawa and Sasaki [1988], and Wegener and Schlegel [1996] propose analytical and numerical modeling schemes to implement the yield surface shape change observations of Phillips and Tang [1972]. After careful scrutiny of these modeling schemes, it has been observed that most of these models use complex and numerically extensive schemes with higher order state tensors. As a result, these models become less attractive (in some cases, impractical) for implementation with a cyclic plasticity model.

Shiratori and his co-workers (Yoshida et. al [1977], Shiratori et. al [1979]), on the other hand, propose a so-called equi-plastic-strain surface that can be used as the plastic potential surface instead of the yield surface generally used in cyclic plasticity modeling. This equi-plastic-strain surface can effectively incorporate the effect of distorted yield surface in the flow rule as this surface and the yield surface have the same normal direction at the current stress point. Experimental results of Yoshida et. al [1977] and Shiratori et. al [1979] also demonstrate the basis behind the applicability of using the equi-plastic-strain surface as the plastic potential surface for incremental plastic strains. Moreover, the formulation for the equi-plastic-strain surface is simpler compared to other deformed yield surface formulations.

Towards developing a generalized ratcheting simulation model, the use of the equi-plastic-strain surface as the plastic potential surface is examined in this study. Some key limitations of the Shiratori et. al [1979] model are identified. Two modeling schemes (models I and II) are developed to eliminate these limitations of the Shiratori et. al [1979] model. These new models are evaluated against a set of biaxial ratcheting experiments on stabilized carbon steels from Hassan and Kyriakides [1992]. Model I predicts nonlinearity in the ratcheting rates for initial cycles, but shakes down at higher cycles (see Fig. 2.4). The model II, on the other hand, simulates almost constant rates of ratcheting and fails to represent the change in the ratcheting rate with variation in the axial strain amplitudes (see Fig. 2.6). Some very critical aspects of modeling like the symmetry direction and the evolution of the isotropic bound need to be verified from experimental observations. This study demonstrates the basic methodology and promise in incorporating the equi-plastic-strain surface as the plastic potential

surface into the cyclic plasticity modeling. However, some experimental studies on the shapes of the equi-plastic-strain surface, especially when unloading occurs far away from the bounding surface, are essential in order to have a more representative modeling scheme.

REFERENCE

Armstrong, P.J. and Frederick, C.O. A Mathematical Representation of the Multiaxial Bauscinger Effect. *CEGB Report* No. RD/B/N 731, 1966.

Bari, S., Hassan. T., (2000a) Anatomy of coupled constitutive models for ratcheting simulation. *International Journal of Plasticity*, Vol 16, pp. 381-409.

Bari, S., Hassan. T., (2000b) Kinematic hardening rules in uncoupled modeling for multiaxial ratcheting simulation. Int. J. Plasticity. (In press)

Bari, S., Hassan. T., (2000c) An advancement in cyclic plasticity modeling for multiaxial ratcheting simulation. Int. J. Plasticity. (In press)

Burlet, H., Cailletaud, G., (1987). Modeling of Cyclic Plasticity in Finite Element Codes. Proc. of 2nd *Int. Conf. on Constitutive Laws for Engineering Materials*: *Theory and Applications*, pp. 1157-1164.

Chaboche, J.L. (1991) On Some Modifications of Kinematic Hardening to Improve the Description of Ratcheting Effects. *International Journal of Plasticity*, Vol 7, pp. 661-678.

Corona, E., Hassan, T. and Kyriakides, S. (1996) On the Performance of Kinematic Hardening Rules in Predicting a Class of Biaxial Ratcheting Histories. *International Journal of Plasticity*, Vol 12, pp. 117-145.

Dafalias, Y.F. and Popov, E.P. (1976) Plastic Internal Variables Formalism of Cyclic Plasticity. *Journal of Applied Mechanics*, Vol 43, pp. 645-650.

Delobelle, P., Robinet, P., Bocher, L,. (1995). Experimental study and phenomenological modelization of ratcheting under uniaxial and biaxial loading on an austenitic stainless steel. *International Journal of Plasticity*, 11, 295-330.

Eisenberg, M.A. and Yen, C.F. (1981) A Theory of Multiaxial Anisotropic Viscoplasticity. *Journal of Applied Mechanics*, Vol 48, pp. 276-284.

Eisenberg, M.A. and Yen, C.F. (1984) The Anisotropic Deformation of Yield Surface. *Journal of Engineering Materials and Technology*, Vol 105, pp. 355-360.

Hassan, T. and Kyriakides, S. (1992) Ratcheting in Cyclic Plasticity, Part I: Uniaxial Behavior. *International Journal of Plasticity*, Vol 8, pp. 91-116.

Hassan, T. and Kyriakides, S. (1994) Ratcheting of Cyclically Hardening and Softening Materials, Part II: Multiaxial Behavior. *International Journal of Plasticity*, Vol 10, pp. 185-212.

Hassan, T., Corona, E. and Kyriakides, S. (1992) Ratcheting in Cyclic Plasticity, Part II: Multiaxial Behavior. International Journal of Plasticity, Vol 8, p. 117-146.

Ilyushin, A.A. (1954) On the Relation Between Stresses and Small Strains in the Mechanics of Continua (in Russian). *Prikl. Mat. Mech*., Vol 18, pp. 641-666.

Ishikawa, H. and Sasaki, K. (1988) Yield Surfaces of SUS 304 Under Cyclic Loading. *Journal of Engineering Materials and Technology*, Vol 110, pp. 365-371.

Kurtyka, T. and Zyczkowski, M. (1996) Evolution Equations For Distortional Plastic Hardening. *International Journal of Plasticity*, Vol 12, pp. 191-213.

Ohno, N. and Wang, J.-D. (1993) Kinematic Hardening Rules with Critical State of Dynamic Recovery, Part I: Formulations and Basic Features for Ratcheting Behavior. *International Journal of Plasticity*, Vol 9, pp. 375-390.

Ortiz, M. and Popov, E.P. (1983) Distortional Hardening Rules for Metal Plasticity. *ASCE Journal of Engineering Mechanics*, Vol 109, pp. 1042-1057.

Phillips, A. and Lu, W.-Y. (1984) An Experimental Investigation of Yield Surfaces And Loading Surfaces of Pure Aluminum With Stress-Controlled And Strain-Controlled Paths of Loading. Journal of Engineering Materials and Technology, *Trans. ASME*, Vol 106, pp. 349-354.

Phillips, A., Lee, C.W., (1979) Yield surfaces and loading surfaces: experiments and recommendations. *International Journal of Solids and Structures*, Vol 15, pp. 715-729.

Phillips, A., Tang, J.-L., (1972) The effect of loading path on the yield surface at elevated temperatures. *International Journal of Solids and Structures*, Vol 8, pp. 463-474.

Shiratori, E., Ikegami, K. and Yoshida, F. (1979) Analysis of Stress-Strain Relations by Use of An Anisotropic Hardening Plastic Potential. *Journal of the Mechanics and Physics of Solids*, Vol 27, pp. 213-229.

Wegener, K. and Schlegel, M. (1996) Suitability of Yield Functions for the Approximation of Subsequent Yield Surfaces. *International Journal of Plasticity*, Vol 12, pp. 1151-1177.

Yoshida, F., Murakami, T., Kaneko, K., Ikegami, K. and Shiratori, E. (1977) Plastic Behaviour in the Combined Loading along Straight Stress Paths With a Bend. *Bulletin of the JSME*, Vol 20, pp. 1549-1556.